16th World Conference on Earthquake, 16WCEE 2017
Santiago Chile, January 9th to 13th 2017
Paper N° 1770
Registration Code: S-S1462989834

EXPERIMENTAL SEISMIC BEHAVIOUR OF A PRECAST INDUSTRIAL BUILDING AT THE CIVIL PROTECTION CENTRE IN FOLIGNO, ITALY

G. Bongiovanni[(1)], G. Buffarini[(1)], P. Clemente[(1)], F. Saitta[(1)],
M. De Angelis[(2)], A. Boccamazzo[(3)], P. Felici[(4)]

[(1)] *ENEA, Casaccia, giovanni.bongiovanni@enea.it, giacomo.buffarini@enea.it, paolo.clemente@enea.it, fernando.saitta@enea.it*
[(2)] *Sapienza Università di Roma, maurizio.deangelis@uniroma1.it*
[(3)] *ENEA, Visiting Engineer, antonioboccamazzo@outlook.it*
[(3)] *Regione Umbria, pfelici@regione.umbria.it*

Abstract

Starting from the bad experience of the May 2012 Emilia-Romagna earthquake, Italy, ENEA and Umbria Region, included also an industrial building among the instrumented structures in the framework of a large research project for the monitoring of the new Civil Protection Centre in Foligno, Italy. The building is about 60x60 m and has the main structure composed of four frames, with five columns and precast beams. The fixed instrumentation, composed of 12 accelerometers connected to an acquisition system, was limited to a single intermediate frame. The accelerometer network was first tested by using a seismometer network for ambient vibration recordings, which also allowed performing the dynamic characterization of the structure. Then several seismic events were recorded and classified on the basis of the input energy at the foot of the structure. Data analyses pointed out changes in the resonance frequencies of the building during each event, probably due to non-linear effects related to the connections between beams and columns and to the contribution of non-structural elements.

Keywords: industrial buildings; experimental analysis; seismic behavior; seismic monitoring.

1 Introduction

During the seismic event of May 2012 in the Emilia-Romagna Region, Italy, several industrial structures collapsed or were severely damaged. They had been built following non-seismic old Italian codes, making use of precast concrete structures. In addition, internal steel shelves exhibited instability in several cases [1][2].

This was only one of the last seismic events that brought to light the key issue of the safety of industrial precast buildings. Since several decades, precast/pre-stressed reinforced concrete (p/p. r.c.) structures represent a widely used typology for industrial facilities and other kinds of commercial destination all over the world. They often showed a good performance under earthquakes, but sometimes their behavior pointed out lacks in seismic codes or bad construction details.

In California, during the January 17th, 1994 Northridge earthquake (M_W=6.7), several parking lots suffered widespread damage or collapse [3], demonstrating the deficiencies in structurer designed before the San Fernando seismic event (M_W=6.6), which struck California in 1971. Among the most famous cases, the Cigna Garage, a multi-storey assemblage of precast and in-situ cast elements, which was very close to the epicenter, whose building connections failed, due to loss of bearing of supporting elements [3]. After the San Fernando earthquake a large revision of the code standards was carried out for various types of buildings.

Also the damage to industrial buildings due to the January 17th, 1995, Great Hanshin-Awaji earthquake (Japan, M_W=6.9) were very heavy and gave an impressive lesson to structural engineers. But it is worth reminding that under the strong ground motion, amplified by the soft soils, and extensive effects of settlement and liquefaction, as well as to the fires, the precast prestressed reinforced concrete structures, located in the most affected area, performed remarkably well [4]. They turned to be newer, high quality, regular shaped construction, designed according to Japanese code, revised in 1981.

Very serious damage was also caused to typical one-storey industrial pre-cast structures in the epicenter area by the August 17th, 1999, Kokaeli earthquake (Turkey, M_W=7.4). The poor details, with particular reference to the inadequate connections (pinned or dowel, simple to realize by the prefabricators) between columns and beams were the main cause of this damage [5][6][7].

Finally, also during the May 12nd, 2008, Wenchuan earthquake (China, M_W=7.9), industrial buildings and facilities in the area near the fault rupture were severely affected [8].

Starting from these experiences, ENEA and Umbria Region, in the framework of a large research project for the monitoring of the Civil Protection Centre in Foligno, Italy, included also an industrial building among the instrumented structures, whose experimental seismic behaviour if the subject of this paper. The building is about 60x60 m and has the main structure composed of four frames, with five columns and precast beams. One intermediate frame was instrumented by means of 12 accelerometers connected to an acquisition system. The accelerometer network was first tested by recording ambient vibrations contemporarily with a seismometer network, which allowed also the dynamic characterization of the structure. Eleven seismic events were recorded and classified according to the input energy at the base of the structure. Data analyses pointed out changes in the resonance frequencies of the building during each event. These were related to non-linear effects probably due to the connections between beams and columns and to the contribution of non-structural elements.

2 The building: description and dynamic characterization

The building under investigation has a squared plan of about 60 m size and a total height of 8.7 m, including the covering structure (Fig. 1). The carrying structure is composed by four frames; each of them has four spans of about 15 m. The precast columns are placed in pocket plinth foundations and have at the top a suitable shape to house the T shape precast beams, connected to them also by means of projecting rebars. The covering is not continuous but composed by concrete elements and alternate to plastic ones, supported by the beams (Figs. 2 and 3).

Each pocket plinth is supported by four piles (diameter 60 cm, length 9.0 m). U beams (30·70 cm) connect the plinths along the perimeter of the building, while rectangular beams (60·25 cm) are between the plinths

inside the building. The perimeter U beams also support the perimeter lightweight concrete panels, so extra plinths (100·100 cm, height 135 cm) supported by one pile (diameter 60 cm, length 9.0 m) are placed between two successive perimeter plinths.

Fig. 1 – The building of the Civil Protection Centre in Foligno, Italy

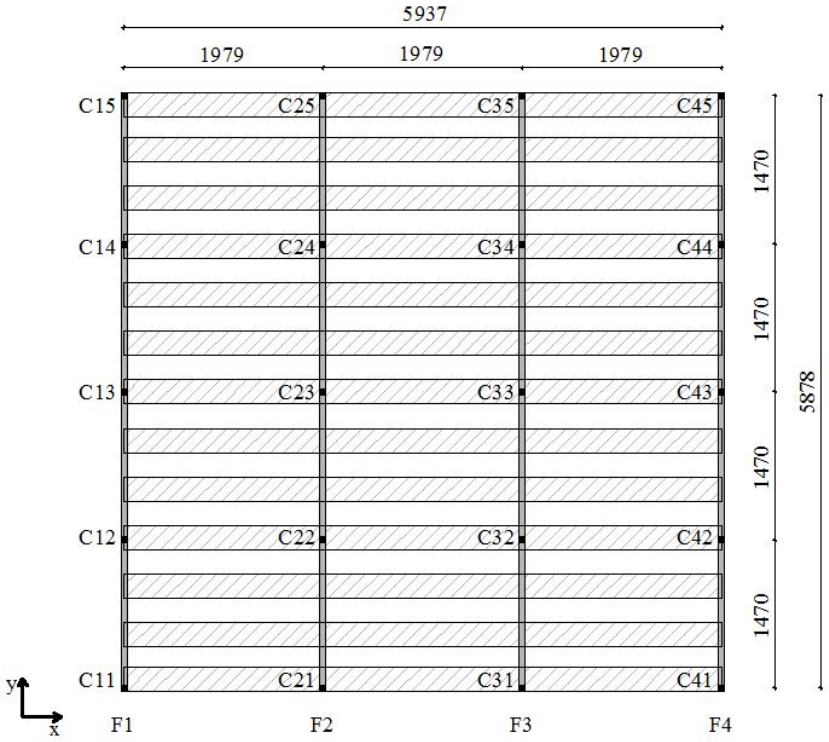

Fig. 2 – Structure of the building with the frames F1 to F4 and the columns (dimensions in cm).

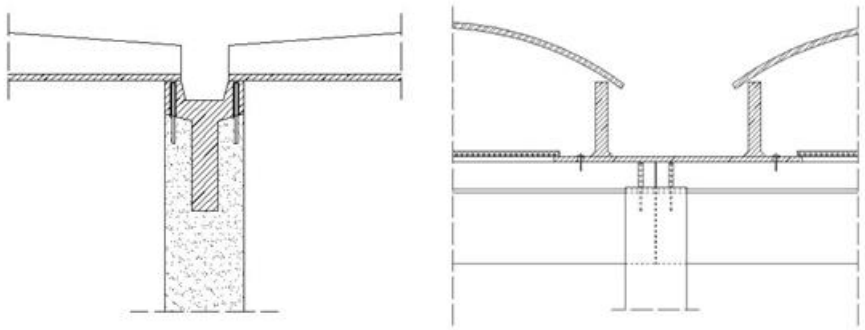

Fig. 3 – Beam-column connection (left) and covering elements-beam connection (right).

In the following the direction of the frames is indicated as y direction or longitudinal direction, while the orthogonal one is called x direction or transversal direction. The frames are numbered from F1 to F4 and, for each of them, the columns from 1 to 5. So the i-th column of the j-th frame is indicated as Cji.

The structure was instrumented by using a K2 acquisition system with an internal triaxial accelerometer and nine uniaxial accelerometers FBA-11 connected to it. These were deployed on the internal frame F2 (Fig. 4). The K2 with the triaxial accelerometer (A01, A02 and A03, respectively) is at the foot of the middle column (column C23), on the foundation plinth. The recorded time histories were assumed to be the input to the frame. Two accelerometers (A11 and A12) are at the base of the external columns, C21 and C25 respectively, in the longitudinal direction. Sensors A04, A05 and A06 are at the top of columns C23, C21 and C25 respectively, in the longitudinal direction. Sensors A09 and A10 are on the beams, very close to A05 and A06. Finally Sensors A07 and A08 are in the transversal direction at the top of columns C21 and C25, respectively.

In order to check the correct working of the accelerometer network, ambient vibrations were recorded also by means of a temporary seismometer array, which were composed of 24 Kinemetrics SS-1 connected to a Granite acquisition system. Ten seismometers (S01 to S08, S11 and S12) were deployed very close to the corresponding accelerometers (A01 to A08, A10 and A12). Furthermore, seven seismometers were deployed on frame F1 (at the base of columns C11 and C15 and at the top of columns C11, C13 and C15) and other seven on frame F3 (at the base of columns C31 and C35 and at the top of columns C31, C33 and C35), i.e., on an external and an internal frame. Fig. 5 shows the location of seismometer S11, close to accelerometer A11 at the base of column C21 (left), and location of accelerometers A08 and A09 with the corresponding seismometers S08 and S09 at the top of column C25 (right).

Ambient vibrations were recorded for 20 min, with a sample ratio of 200 samples/s (Δt = 0.005 s) equal to that of the accelerometer network. The recorded accelerations, obtained from the fixed instrumentation, were integrated to be compared with those obtained from the seismometers. The comparison was carried out both in time and frequency domain. Furthermore, the dynamic characterization of the building was also performed, extracting the resonance frequencies, modal shapes and damping.

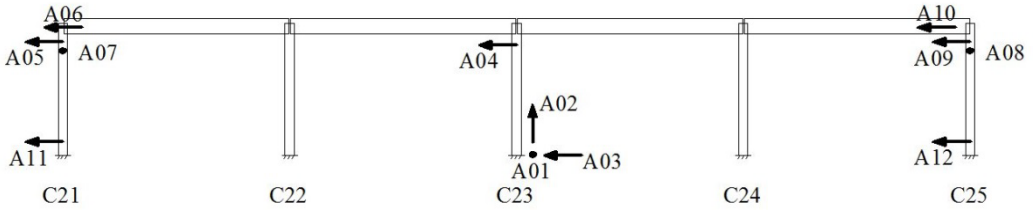

Fig. 4 – Accelerometer locations on frame F2.

Fig. 5 – Location of accelerometer A11 and seismometer S11 (left) and location of accelerometers A08 and A09 and seismometers S08 and S09 (right) on frame F2.

The comparison between the sensors at the base of the columns in the time domain showed some differences due to distance between the corresponding sensors. A very good agreement was obtained between seismometers and accelerometers placed at the top of the columns.

The spectral analysis in the longitudinal direction showed four peaks in a narrow range around 2.0 Hz. A detailed analysis about this occurrence showed that these resonances are associated to the same modal shape, whose frequency varies during the recording. In this mode the side frames, F1 and F4, show displacements lower than those of the internal frames, F2 and F3, as shown in Fig. 6, where spectral amplitudes at 2.05 Hz were considered. This higher stiffness of the side frames with respect to the internal ones can be obviously related to the presence of the external panels. Other peaks are at about 4.0 Hz with amplitude much lower. The cross analysis showed that the recordings of the same frame are always in phase but the signals of different frames showed non-significant values of the phase factor.

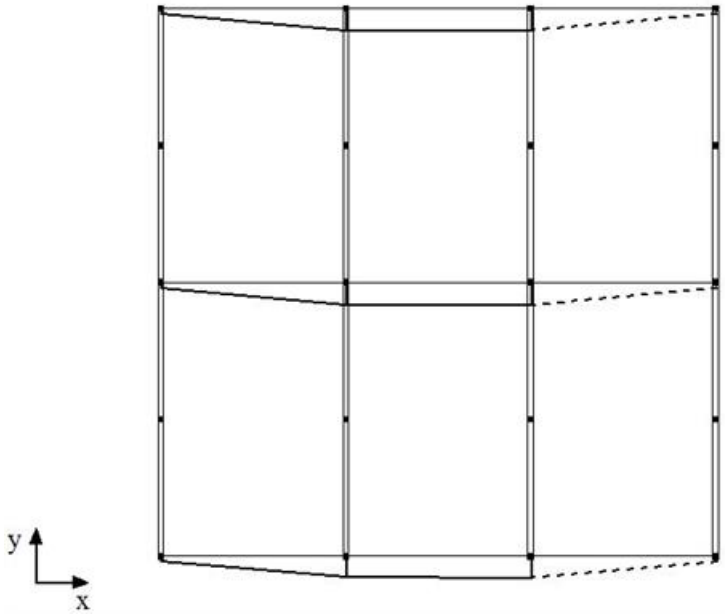

Fig. 6 – Modal shape in the longitudinal direction at the three transversal alignments considered (the amplitudes of F4 were assumed equal to those at the corresponding location of F1).

3 Earthquake events recorded

Eleven seismic events were recorded from November 2014 to September 2015. They were classified on the basis of the Arias intensity I_A measured at the base of the building by the accelerometers A01, A02 and A03 [9]:

$$I_A = \frac{\pi}{2g}\int_0^T \left(a_{A01}^2 + a_{A02}^2 + a_{A03}^2\right)dt \quad (1)$$

The events are listed in Table 1 with their main characteristics. All the events present similar duration and energy content.

The frequency domain analysis allowed determining the first resonance frequencies in all the events. The values determined by using two well-known different methods, the Peak Picking and the Frequency Domain Decomposition [10], which gave very similar results. These are plotted in Fig. 7, for the frequency in transversal and longitudinal direction, respectively. The first varies from the maximum one, obtained in the ambient vibration test and equal to 1.92 Hz, to a minimum value of 1.65 Hz. The second varies from the maximum of 2.05 Hz relative to the ambient vibrations, to a minimum of 1.80 Hz. The resonance frequencies observed during the seismic events were always lower than those of the ambient vibration test. Each event gave different reduction of the two frequencies and the maximum reductions were not observed in the same event.

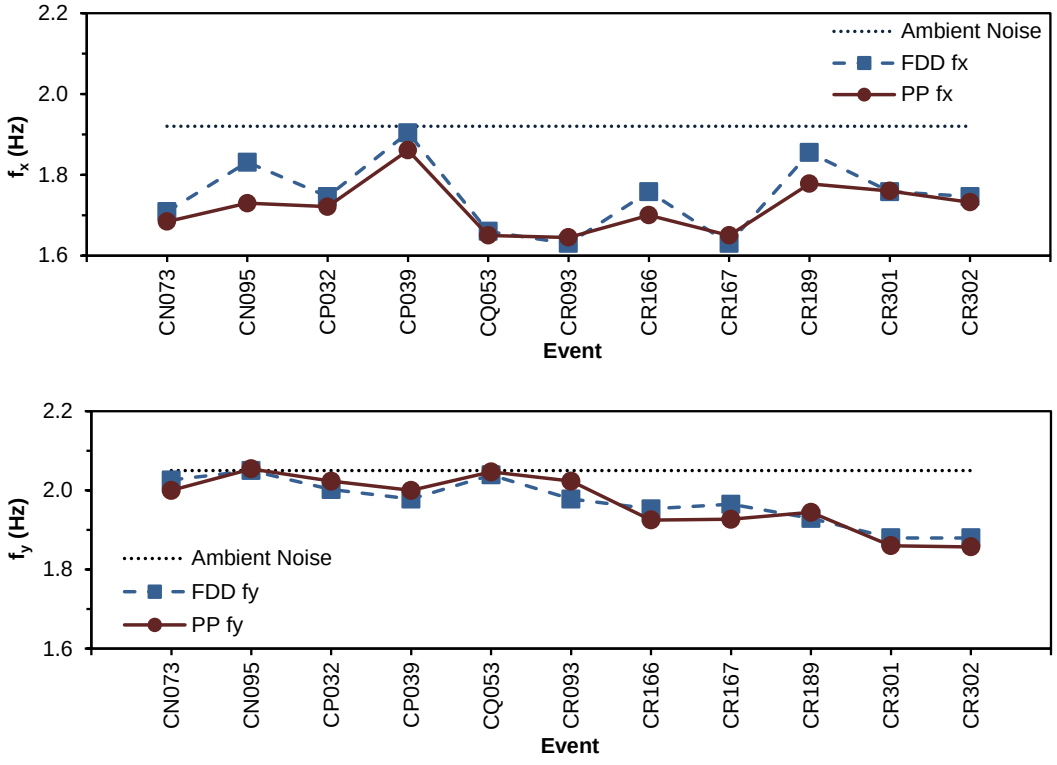

Fig. 7 – First transversal resonance frequency (up) and first longitudinal resonance frequency (down) in the recorded seismic events.

The variation of the resonance frequencies during the event induced to perform a more detailed analysis of the accelerometer time histories. Each time history was first divided into three parts, the pre-event, the event and the post-event. These were individualised by means of the energy ratio I/I_A between the energy I at the generic time t and the Arias intensity at the base of the buildings. In more details the strong phase was assumed to start at

the time when I/I_A = 0.05 and to end when I/I_A = 0.95 [11]. In Fig. 8 the three parts are individualised for each event and in Fig. 9 the first longitudinal resonance frequencies in the pre-events and in the post-events are plotted. As one can see the resonance frequency in the post-event is always equal or very close to that of the ambient analysis. This occurrence implies that the effects of the earthquakes, probably related to nonlinear response under seismic actions, were reversible and the structure recovered the previous dynamic characteristics. The damping varied between the minimum one observed during the ambient vibration analysis (4.4% in the transversal x direction, 4.8% in the longitudinal y direction) up to about 9.5% observed in both the directions.

Table 1 – Earthquakes recorded.

Earth. No.	Date	Time	M_w	Depth (km)	Epicentral distance (km)	I_A
CN073	23.11.2014	01:37:31	1.2	9.0	14	2.47E-04
CN095	08.12.2014	22:50:37	1.6	7.6	20	1.54E-04
CP032	04.08.2015	14:22:09	3.2	9.0	48	6.12E-04
CP039	04.15.2015	01:36:45	2.9	8.2	50	7.66E-05
CQ053	05.21.2015	09:33:45	3.4	24.2	47	9.10E-04
CR093	25.07.2015	20:57:50	3.0	9.7	45	5.58E-04
CR166	15.08.2015	16:59:05	2.7	9.6	33	4.25E-04
CR167	15.08.2015	17:51:16	2.9	9.7	33	5.27E-04
CR189	24.08.2015	21:13:11	1.7	9.9	6	4.10E-04
CR301	18.09.2015	19:24:53	3.5	8.9	80	1.84E-04
CR302	19.09.2015	-	-	-	-	9.59E-04

On the time histories filtered in the range of interest [1.8, 2.2] the instantaneous frequency obtained by means of the Hilbert transform was calculated (Fig. 10) [12][13]. In the same figure also the spectrogram obtained dividing the time length of the recorded time history into eight portions is plotted.

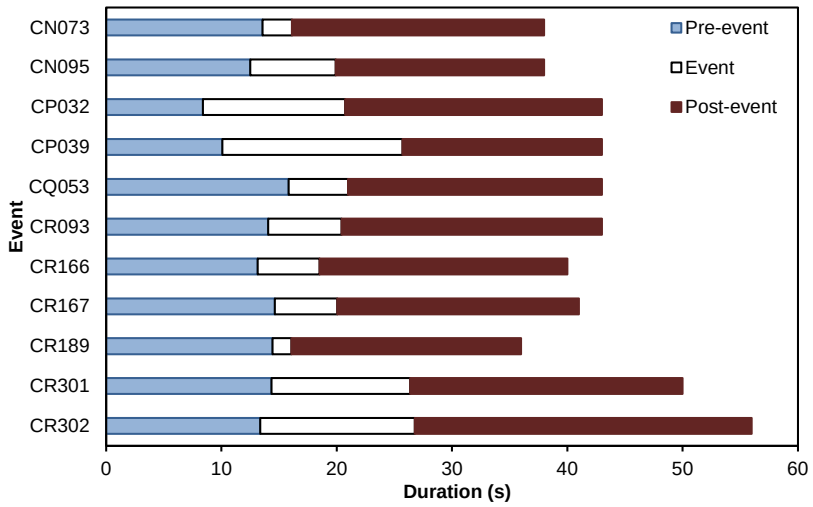

Fig. 8 – Pre-event, event and post-event in the recorded earthquakes.

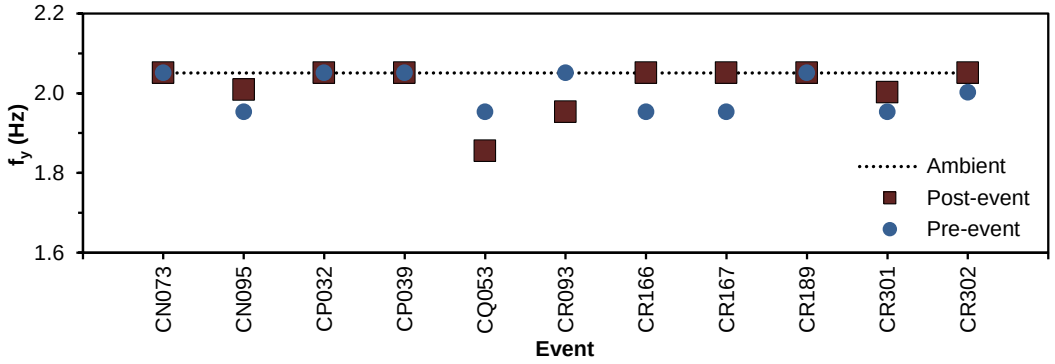

Fig. 9 – First longitudinal resonance frequencies in the pre- and post-events compared with that obtained from the ambient vibrations.

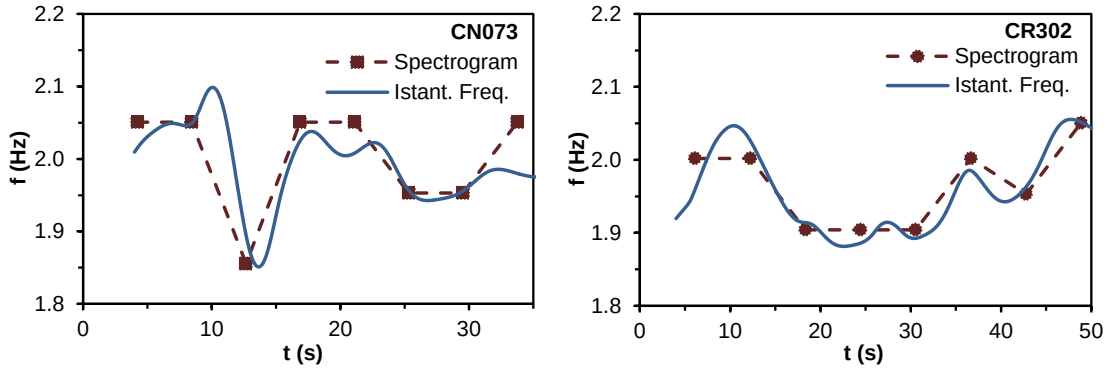

Fig. 10 – Variation of the first longitudinal frequency during event CN073 (left) and event CR302 (right).

The percentage difference between the minimum and the maximum frequencies for each event are plotted in Fig. 11 for the transversal direction (left) and the longitudinal direction (right). The reduction with the increases of the input energy, between 5% and almost 15% for the transversal frequency, is apparent. These values are usually associated to important damage in a structure [14]. Anyway, in this case the structure recovered its resonance frequency, demonstrating not to have been irreversibly damaged by the successive earthquakes.

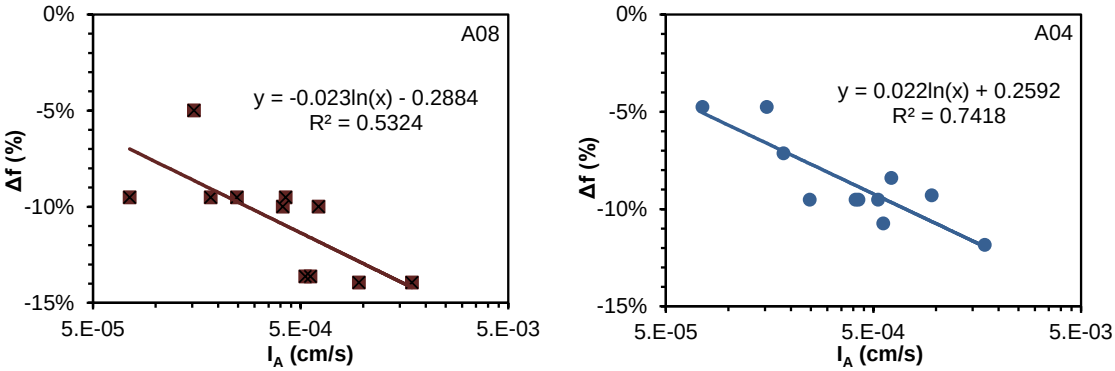

Fig. 11 – Percentage reduction of the first transversal resonance frequency versus I_A (A08, left) and of the first longitudinal resonance frequency versus I_A (A04, right).

The variations of the resonance frequencies are certainly due to nonlinear effects. These could be related to the several causes, among these the non-rigid connection between beams and columns as demonstrated by the acceleration time histories recorded at two very close locations on the column (A05) and on the beam (A06), respectively (Fig. 12). In the case on the left (CR302), the two time histories show low discrepancies in the peak amplitudes, while in the case on the right (CR189) they present also phase shifts.

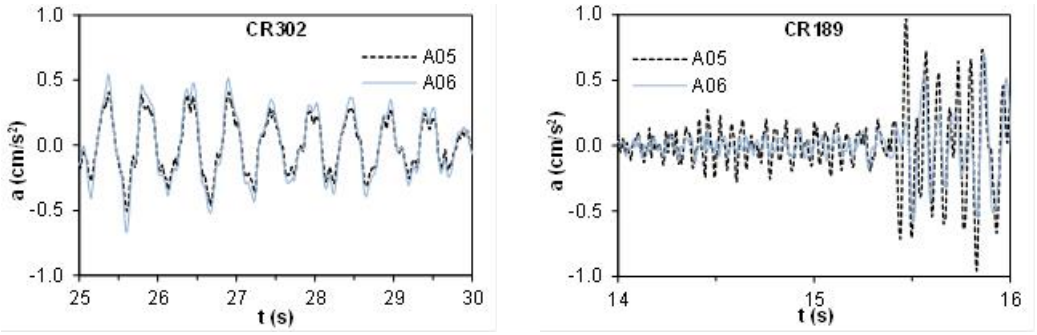

Fig. 12 – Comparison between the recorded acceleration time histories on the column (A05) and on the beam (A06) for events CR302 (left) and CR189 (right).

4 Numerical modelling

A first numerical model was set up based on the original design and an accurate visual inspection, by using the computer code SAP2000. The columns were considered fully fixed at their base, while the concrete elements of the covering were supposed to be connected to the beams by means of cylindrical hinges. These allow only flexural rotations around the horizontal axis, parallel to y.

The panels played an important role in the dynamic characteristics of the building. If their contribution in terms of mass are considered but their stiffness is neglected, the structures presents three decoupled modal shapes. The first two are translational modes along the main axes, respectively, the third one is torsional. Furthermore, the translational frequencies would be quite lower than the experimental ones, also considering a wide range of variability of the mechanical characteristics of the materials.

So the model was improved first of all including the stiffness contribution of the panels (Fig. 13), and modal shapes very similar to those of the ambient vibration analysis were obtained. The connections between the perimeter panels and the beams were modelled as rigid.

The model accounts for the effective stiffness of the covering elements because these are not continuous and the floor cannot be assumed to be rigid. Also the connections between the concrete covering elements and the beams were modelled as rigid.

A suitable corresponding between the resonance frequencies was obtained by changing the mass and the stiffness of the perimeter panels by using a procedure of sensitivity analysis and model updating. In more details, these were supposed to have a constant thickness equal to the total one, a range of variability for the mass density ρ and the Young's modulus E was first defined and then the influence of their changes in these ranges was analysed. Finally the average value of the mass density $\rho = 18.5$ kN/m^3 was chosen and the curve relative to the variability of the stiffness was simulated by means of the variation of the Young's modulus E, extracting the value for which the differences in terms of resonance frequencies and modal shapes were minimum (Fig. 14) according to the relation [10]:

$$\varepsilon\left(f_{mi},\phi_i\right)=\sum_{i=1}^{2}\left[\alpha\left(\frac{f_{mi}-f_{ei}}{f_{mi}}\right)^2+\beta\left(\frac{1-\sqrt{MAC_i}}{MAC_i}\right)^2\right] \quad (2)$$

with α=0.6 and β=0.4. In this way the numerical frequencies f_n were quite similar to the experimental frequencies f_e (Table 2) and the torsional mode was associated to a very high frequency, which was not found in the experimental results.

The Young's modulus E obtained from this analysis is to be considered consistent with the typical geometrical and mechanical characteristics of the panels, taking into account that these represents average values of the lightweight concrete panels.

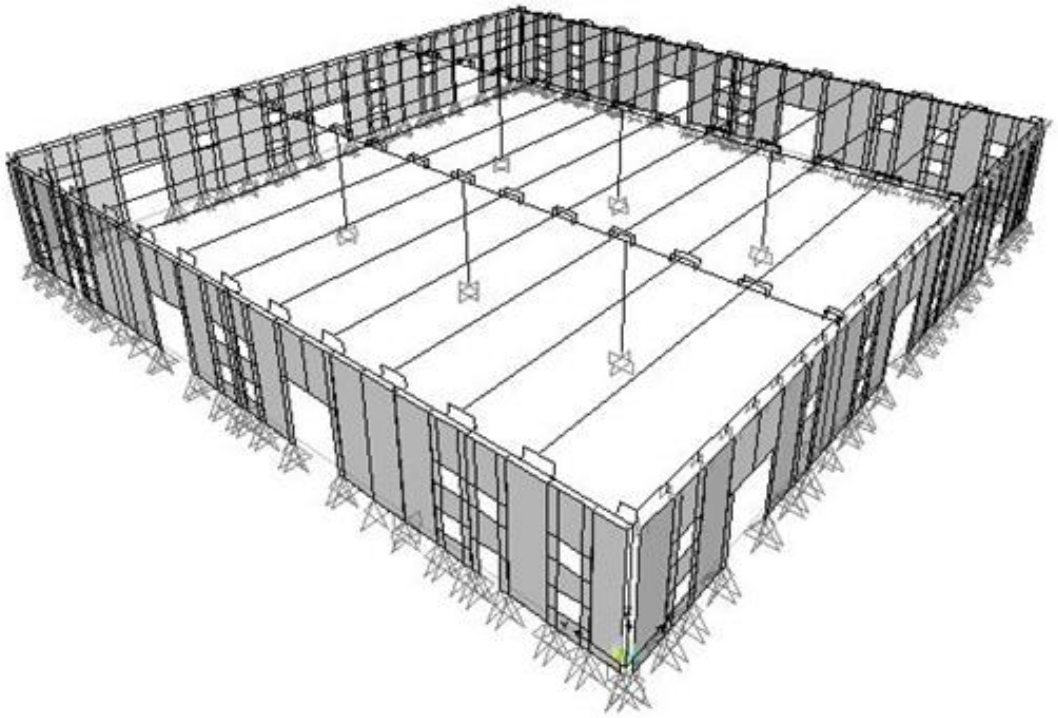

Fig. 13 – Finite element model.

Table 2 – Experimental and numerical frequencies

Mode	f_e (Hz)	f_n (Hz)	MAC
1	1.92	1.92	0.994
2	2.05	2.05	0.998

5 Conclusions and future developments

The experimental seismic analysis of the precast industrial building of the Civil Protection Centre at Foligno pointed out the first two translational frequencies and the associated modal shapes. The variations of the resonance frequencies observed during the seismic events recordings, which reached values up to 10% in the longitudinal direction and up to 15% in the transversal one with reference to the maximum values observed in the ambient test, are to be expected in structures of this type, in which the contribution of the non-structural

elements could be very important. In the studied building the contribution of the perimeter panels turned out to have an important influence on the structural behaviour. The structure always recovered the resonance frequency found under ambient vibrations, demonstrating not to have been irreversibly damaged by the earthquakes. Anyway, a rule valid in general was not found and a more detailed analysis should be done, which accounts for several parameters, among these the input energy during each event it and of the different frequency content.

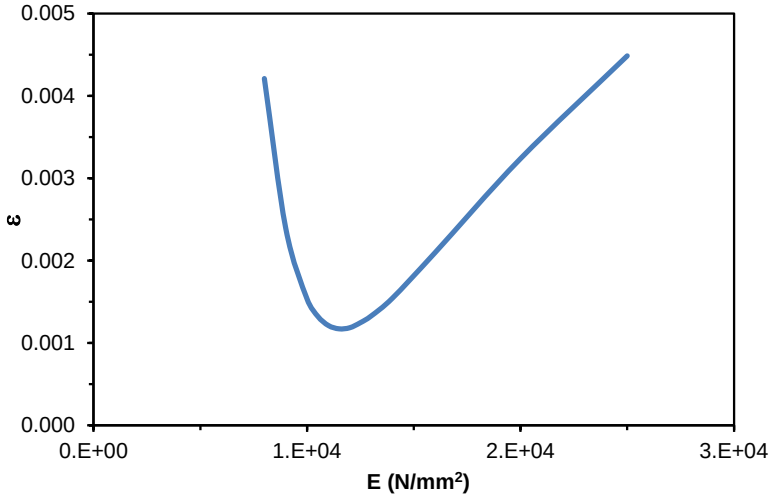

Fig. 14 – ε versus the Young's modulus E for mass density ρ = 18.5 kN/m^3.

The finite element model was set up first on the basis of the original design and of the visual inspection and then on the basis of the experimental results. It gave very good results in terms of dynamic characteristics of the building.

Future developments of this study must be the improvement of the model, with particular reference to the connections between the concrete covering elements and the beams, between the beams and the columns and also between the columns and the pocket plinths. The soil-structure interaction could also play an important role. These aspects can be analysed if other data will be available, relative to the structural behaviour under events of different energy.

Acknowledgements

This paper is part of a research project organized by ENEA in collaboration with the Umbria Region for the seismic monitoring of three buildings of the Civil Protection Centre at Foligno, Italy. The study here described was carried out also in the framework of a scientific collaboration between ENEA and the *Dipartimento di Ingegneria Strutturale e Geotecnica* of *Sapienza Università* of Rome.

References

[1] Saitta F, Bongiovanni G, Buffarini G, Clemente P, Martelli A, Marzo A, Marghella G, Indirli M, Poggianti A (2012): Behaviour of industrial buildings in the Pianura Padana Emiliana earthquake. In *Focus on The Pianura Padana Emiliane Earthquake - Energia, Ambiente e Innovazione*, **4-5**(II), 47-57, ENEA.

[2] Paolini S, Martini G, Carpani B, Forni M, Bongiovanni G, Clemente P, Rinaldis D, Verrubbi V (2012): The May 2012 seismic sequence in Pianura Padana Emiliana: Hazard, Historical seismicity and preliminary analysis of accelerometric records. *Energia Ambiente e Innovazione*, **4-5**(II), 6-22, ENEA.

[3] EERI (1994): Northridge Earthquake January 17, 1994. *EERI Preliminary Reconnaissance Report*, Earthquake Engineering Research Institute.

[4] Muguruma H, Nishiyama M, Watanabe F (1995): Lessons learned from Kobe earthquake, A Japanese perspective. *PCI Journal*, **40**(4), 28-42.

[5] Senel S M, and Kayhan A H (2010): Fragility based damage assessment in existing precast industrial buildings: A case study for Turkey. *Structural Engineering and Mechanics*, **34**(1), 39-60.

[6] Saatcioglu M, Mitchell D, Tinawi R, Gardner N J, Gillies AG, Ghobarah A, Anderson D L, and Lau D (2001): The August 17, 1999, Kocaeli (Turkey) earthquake-damage to structures. *Canadian Journal of Civil Engineering*, **28**(4), 715–737.

[7] Posada M, Wood S L (2002): Seismic performance of precast industrial buildings in Turkey. *Proc. of the 7th U.S. National Conference on Earthquake Engineering*, Boston, USA.

[8] Zhaoa B, Taucera F, Rossetto T (2009): Field investigation on the performance of building structures during the 12 May 2008 Wenchuan earthquake in China. *Engineering Structures*, **31**, 1707–1723.

[9] Arias A (1970): A measure of earthquake intensity. In Hansen R. (ed), *Seismic Design of Nuclear Power Plant*, MIT Press, Cambridge.

[10] Ewins D J (2003): *Modal Testing: Theory, Practice and Application*. John Wiley & Sons.

[11] Trifunac M D, Brady A G (1975): A study on duration of strong earthquake ground motion. *Bulletin Seismological Society of America*, **65**, 581-626.

[12] Kanasewich E R (1981): *Time Sequence Analysis in Geophysics*. Edmonton: The University of Alberta Press.

[13] Bendat J S, Piersol A G. (2011): *Random data: analysis and measurement procedures*. John Wiley & Sons.

[14] Salawu O S (1997): Detection of structural damage though changes in frequency: A review. *Engineering Structures*, **216**, 791-808.